Ab initio study of neutral $(TiO_2)_n$ clusters and their interactions with water and transition metal atoms

2012 J. Phys.: Condens. Matter 24 305301

(http://iopscience.iop.org/0953-8984/24/30/305301)

IOP PUBLISHING JOURNAL OF PHYSICS: CONDENSED MATTER

J. Phys.: Condens. Matter **24** (2012) 305301 (13pp) doi:10.1088/0953-8984/24/30/305301

Ab initio study of neutral $(TiO_2)_n$ clusters and their interactions with water and transition metal atoms

D Çakır[1] **and O Gülseren**

Department of Physics, Bilkent University, Ankara 06800, Turkey

E-mail: gulseren@fen.bilkent.edu.tr

Received 18 February 2012, in final form 15 May 2012
Published 4 July 2012
Online at stacks.iop.org/JPhysCM/24/305301

Abstract

We have systematically investigated the growth behavior and stability of small stoichiometric $(TiO_2)_n$ ($n = 1$–10) clusters as well as their structural, electronic and magnetic properties by using the first-principles plane wave pseudopotential method within density functional theory. In order to find out the ground state geometries, a large number of initial cluster structures for each n has been searched via total energy calculations. Generally, the ground state structures for the case of $n = 1$–9 clusters have at least one monovalent O atom, which only binds to a single Ti atom. However, the most stable structure of the $n = 10$ cluster does not have any monovalent O atom. On the other hand, Ti atoms are at least fourfold coordinated for the ground state structures for $n \geq 4$ clusters. Our calculations have revealed that clusters prefer to form three-dimensional structures. Furthermore, all these stoichiometric clusters have nonmagnetic ground state. The formation energy and the highest occupied molecular orbital (HOMO)–lowest unoccupied molecular orbital (LUMO) gap for the most stable structure of $(TiO_2)_n$ clusters for each n have also been calculated. The formation energy and hence the stability increases as the cluster size grows. In addition, the interactions between the ground state structure of the $(TiO_2)_n$ cluster and a single water molecule have been studied. The binding energy (E_b) of the H_2O molecule exhibits an oscillatory behavior with the size of the clusters. A single water molecule preferably binds to the cluster Ti atom through its oxygen atom, resulting an average binding energy of 1.1 eV. We have also reported the interaction of the selected clusters ($n = 3$, 4, 10) with multiple water molecules. We have found that additional water molecules lead to a decrease in the binding energy of these molecules to the $(TiO_2)_n$ clusters. Finally, the adsorption of transition metal (TM) atoms (V, Co and Pt) on the $n = 10$ cluster has been investigated for possible functionalization. All these elements interact strongly with this cluster, and a permanent magnetic moment is induced upon adsorption of Co and V atoms. We have observed gap localized TM states leading to significant HOMO–LUMO gap narrowing, which is essential to achieve visible light response for the efficient use of TiO_2 based materials. In this way, electronic and optical as well as magnetic properties of TiO_2 materials can be modulated by using the appropriate adsorbate atoms.

(Some figures may appear in colour only in the online journal)

1. Introduction

Titanium dioxide (TiO_2) has been a focus of attention because of its low cost, long-standing stability, catalytically active surfaces and environmental compatibility [1–3]. It has been widely used in many promising applications including production of hydrogen from water and solar energy, solar cells (as an active semiconductor metal oxide in the Grätzel solar cell) [4–8], sensors [9], cleaning of water and air from organic contaminants [1, 10, 11], and photocatalysis [12–15]. Naturally, TiO_2 exists in three different crystal structures as rutile, anatase and brookite. Although rutile crystal is

[1] Present address: Faculty of Science and Technology and MESA$^+$ Institute for Nanotechnology, University of Twente, PO Box 217, 7500 AE Enschede, The Netherlands.

the thermodynamically most stable phase under ambient conditions, the anatase phase becomes more stable than the rutile phase [3] for the nanoparticles smaller than 14 nm. TiO_2 is a large band gap semiconductor (3 eV for rutile and 3.2 eV for anatase) [16, 17] and absorbs only the ultraviolet (down to ∼400 nm) portion of the solar spectrum. Most of the technological applications such as photovoltaics and photocatalysis of TiO_2 are mainly related to its optical properties. However, fully efficient use of TiO_2 materials in these applications is limited because of its wide band gap. There have been several attempts to obtain a band gap narrowing and visible light activity of TiO_2 based systems through doping or substitution with metallic as well as nonmetallic elements [18, 19]. Metal doped TiO_2 prepared by ion implantation with various transition metal (TM) atoms such as V, Cr, Mn, Fe, and Ni has been found to have a large shift in the absorption band toward the visible light region [20–25]. The desired band gap narrowing and enhancement in visible light activity of TiO_2 can also be achieved by using suitable nonmetallic elements such as C, N, F, P, and S [26–32].

The physical and chemical properties of TiO_2 nanomaterials, namely nanowires, nanoparticles and clusters, might be different from those of bulk titania [33]. In general, the ratio of surface to volume atoms increases as the cluster size decreases; accordingly, smaller TiO_2 nanoparticles have more active sites, regarding the photocatalytic applications, because of the high density of surface corner and edge atoms. For example, it has been reported that the catalytic activity of the TiO_2 materials is enhanced as the size and the dimension of these materials decrease [34]. Hence, TiO_2 clusters serve as a model system to understand the photocatalytic and photovoltaic processes, and the nucleation of larger particles. Due to their scientific and technological importance, there are several experimental [35–44] and theoretical studies on small neutral, negatively and positively charged TiO_2 clusters [45–65] and nanoparticles [66–69]. This quite extensive list of theoretical investigations by using density functional based methods can be summarized as follows: for example, Walsh *et al* [47] have studied the structure, stability and electron affinities of TiO_n and TiO_n^- clusters for $n = 1$–3. Stoichiometric and non-stoichiometric (O rich) small neutral and charged clusters have been investigated by Albaret *et al* [48–50]. The relative stability of the various isomers in terms of competition between ionic and covalent effects in Ti–O bonds, electron affinities and optical excitation gaps have been calculated. Jeong *et al* [51] have studied the energetics, equilibrium geometry, and harmonic vibrational frequencies of isolated Ti_mO_n clusters for $m = 1$–6 and $n = 1$–12 by using Gaussian94 based on DFT. Hamad *et al* [52] have searched a large number of cluster geometries making use of interatomic potential to find the global minima of small $(TiO_2)_n$ clusters and the most energetic structures have been reoptimized by using DFT/B3LYP to obtain more accurate results. Furthermore, structural, electronic, and vibrational properties and stabilities of $(TiO_2)_n$ ($n = 1$–8) clusters have been studied by employing DFT based methods [53]. Similarly, Qu *et al* [54, 55] have investigated the electronic structure and the stability of both neutral and singly charged $(TiO_2)_n$ ($n = 1$–9 and 10–16) clusters by using the density functional B3LYP/LANL2DZ method. $(TiO_2)_n$ anatase-like clusters with varying n values between 16 and 32 have been constructed by introducing rigid criteria of stoichiometry, high coordination and balanced charge distribution using the B3LYP method [56]. Besides, Barnard *et al* [58] have studied the electronic and structural properties of anatase TiO_2 nanoparticles through the self-consistent tight binding method and DFT. The reactivity and the structure of small size clusters with $(TiO_2)_n$ ($n = 1$–10) has been investigated by using B3LYP calculations [60, 61]. In this study, acidic and basic properties of the most stable structures of the titania clusters with different sizes have been analyzed by considering the H^+ interaction with the O site for the acidity test and the NH_3 molecule interaction with the Ti site for the basicity test. Likewise, there are several studies investigating the larger TiO_2 nanoparticles [70, 71]. In contrast to small clusters, the structures of large TiO_2 nanoparticles are governed from bulk rutile or anatase phases. However, the structure of small TiO_2 clusters does not look like either anatase or rutile structure, and the average coordination numbers of Ti and O atoms are smaller than the coordination numbers in bulk phases (6 and 3 for Ti and O, respectively).

One of the most important applications of TiO_2 is water splitting and hydrogen production via photovoltaics. There are several theoretical studies on interaction of water with TiO_2 nanoparticles which have different sizes and structures [63, 72–76]. Erdin *et al* [74] have studied the interaction of water with rutile and anatase nanoparticles using tight binding molecular dynamics (MD). Nanoparticles expand in water because of this interaction and water molecules dissociate on the nanoparticle surface. Similarly, Koparde *et al* [75] have performed MD calculations in order to study the interaction of water with anatase and rutile particles ranging from 2.5 to 4 nm at room temperature and hydrothermal conditions.

Concerning the possible use of TiO_2 clusters in wide ranging technological applications including dye-sensitized solar cells, gas sensing, production of hydrogen from water, disinfection of contaminated water and air, self-cleaning coatings, spintronics and photocatalysis, it is essential to know their physical and chemical properties, so one can design and optimize effective applications. Because of their importance for both fundamental science and practical applications, we have presented a systematic investigation of the stability, structural, electronic and magnetic properties of $(TiO_2)_n$ clusters ($n = 1$–10) within DFT. Interaction of these clusters with molecular and atomic species, namely H_2O, Co, V, and Pt, has also been studied. The aim of this study is to elucidate how TiO_2 based materials behave in low dimensions. The paper is organized as follows. After summarizing the general properties of TiO_2 nanoparticles and reviewing the comprehensive list of their theoretical investigation based on density functional theory in section 1, we first outline the computational methods in section 2. Then, we present the results on the structure of $(TiO_2)_n$ ($n = 1$–10) clusters and discuss their stability and the electronic structure in section 3. This section is divided into two more subsections, section 3.5

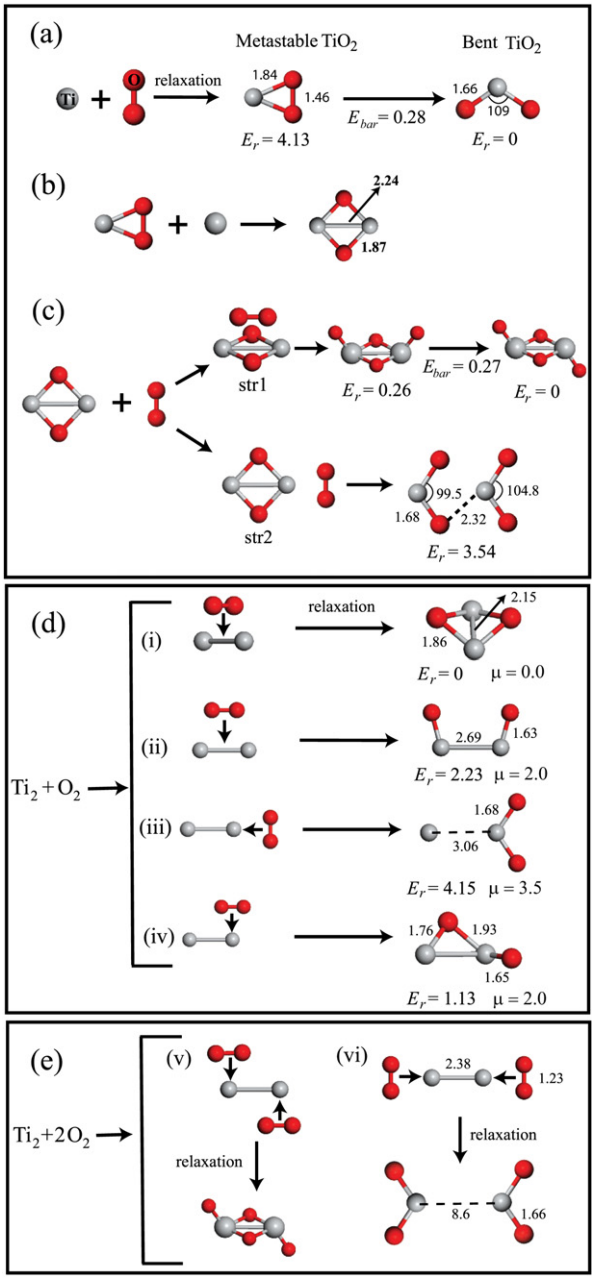

Figure 1. Growth mechanism of some small TiO and TiO_2 molecules. Light (gray) and dark (red) balls are used to represent Ti and O atoms, respectively. Bond lengths between corresponding atoms and magnetic moments μ are given in Å and μ_B, respectively. E_r (in eV) represents the relative energy of a particular cluster with respect to its ground state isomer. E_{bar} is the energy barrier between two corresponding structures in eV.

and section 3.6, in which the water and the transition metal adsorption to the $(TiO_2)_n$ clusters are discussed, respectively. Lastly, we conclude briefly in section 4.

2. Computational method

We have performed first-principles plane wave calculations [77, 78] within density functional theory (DFT) [79] using projector augmented-wave (PAW) potentials [80, 81]. $3p^6 3d^3 4s^1$ for Ti and the $2s^2 2p^4$ electronic configuration for the O atom have been used in the pseudopotentials. The exchange–correlation potential has been approximated by the generalized gradient approximation (GGA) using the PW91 [82] formulation. All structures have been treated in a tetragonal supercell (with lattice parameters a_{sc}, b_{sc} and c_{sc}) using periodic boundary conditions. To prevent interaction between adjacent isolated clusters, a large spacing between the clusters (at least 10 Å) has been introduced. In the self-consistent potential and total energy calculations, only the Γ point has been used for $\boldsymbol{k}$-point sampling [83]. A plane wave basis set with kinetic energy cutoff (E_{cut}) 500 eV has been used. All atomic positions have been optimized by using the conjugate gradient method where total energy and forces on each of the atoms are minimized. The convergence criterion for energy and forces has been chosen as 10^{-5} eV between two ionic steps, and the maximum force allowed on each atom is 0.03 eV $Å^{-1}$. The Gaussian smearing method [84] has been used and the width of smearing has been chosen as 0.05 eV.

3. Results and discussion

In order to test the reliability of our calculations, we have calculated the structural parameters of rutile and anatase bulk crystals of TiO_2 as well as the structural and magnetic properties of TiO and TiO_2 molecules. We have compared these calculated results with available experimental data. The lattice parameters a and c of rutile are 4.64 (4.59) and 2.97 (2.96) Å, respectively. The experimental values [85–87] are quoted in parentheses. For the case of the anatase phase, a and c values are 3.8 (3.79) and 9.70 (9.51) Å, which are in fair agreement with experimental values [86, 87]. The TiO molecule prefers the magnetic ground state with a magnetic moment of $\mu = 2\mu_B$ and the Ti–O bond length is 1.63 Å, in good agreement with the experimental value [88]. The bent TiO_2 molecule, which has the same structure as the water molecule, is about 2 eV energetically more stable than its linear structure isomer, and both of them prefer the singlet state. The Ti–O bond length and O–Ti–O bond angle are 1.66 Å and 109°, respectively. The experimentally [35] estimated value of O–Ti–O angle is 110± 5. The linear Ti–O–O–Ti structure is unstable; relaxation leads to formation of two separated and weakly interacting TiO molecules through the broken O–O bond. It is obvious that the bent TiO_2 molecule is the smallest stoichiometric titanium dioxide cluster. We can propose a formation mechanism for this bent TiO_2 molecule by using only a single Ti atom and O_2 molecule. In figure 1(a), we have shown the formation sequence and structural parameters of this bent TiO_2 molecule. As a result of the interaction between the Ti atom and O_2 molecule, first we have obtained a metastable structure in which the O–Ti–O bond angle and Ti–O and O–O interatomic distances are 46.9°and 1.84 and 1.46 Å, respectively. O_2 binds to the Ti atom as a molecule. However, the O–O bond significantly elongates due to interaction with Ti. Furthermore, the total energy of the bent structure is 4.13 eV lower than that of the metastable one, and the energy barrier between these two structures is calculated as 0.28 eV.

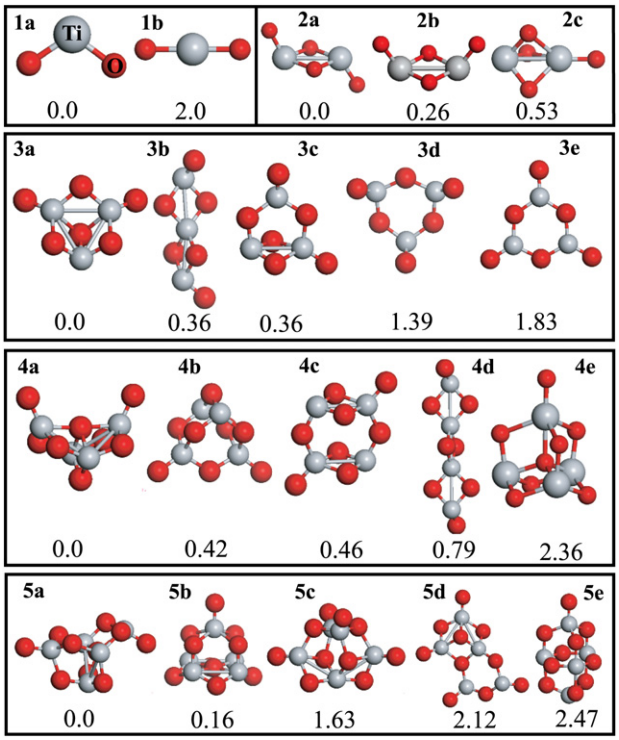

Figure 2. Structure of the five lowest lying isomers of the neutral $(TiO_2)_n$ clusters, where $n = 1$–5. Assigned labels are indicated in order to identify each of the clusters. **na**, **nb**, etc, are the isomers of $(TiO_2)_n$ clusters. Ti and O atoms are demonstrated by light (gray) and dark (red) spheres, respectively. The energies (in eV) relative to the corresponding ground state geometries (**na**) are also given.

Figures 1(b)–(e) represent the formation path of some other small TiO and TiO_2 clusters. When an extra Ti atom is placed close to this metastable TiO_2 cluster, the O–O bond is completely broken as a consequence of interaction with this additional Ti atom, and the emergent Ti_2O_2 molecule has singlet ground state and planar geometry as displayed in figure 1(b). Ti–Ti and Ti–O bond lengths become 2.24 and 1.87 Å, respectively. In figure 1(c), we have illustrated the interaction of this Ti_2O_2 cluster with a single O_2 molecule. Two possible interaction structures, namely str1 and str2, have been investigated. In the former case, we have obtained a Ti_2O_4 cluster. Upon relaxation of str2, two separated bent TiO_2 clusters have been formed. The formation of the Ti_2O_4 cluster is 3.28 eV more energetic than that of two bent TiO_2 clusters.

One can also imagine that formation of small TiO and TiO_2 clusters from Ti and O dimers might be possible. We have considered four initial structures to simulate reaction between Ti_2 and O_2 as depicted in figure 1(d). In general, magnetic clusters have been formed upon the interaction of Ti and O dimers. All these non-stoichiometric magnetic clusters have at least one onefold coordinated or monovalent O atom. However, the ground state structure is nonmagnetic and has no monovalent O atom. In contrast to interaction of the Ti atom with the O_2 molecule (see figure 1(a)), the O_2 molecule dissociates after reaction with the Ti_2 molecule. Interestingly, there is no energy barrier for this dissociation. As a result of the breaking of the O–O bond (which occurs in all proposed interaction cases between Ti and O dimers, represented in figure 1(d)(i–iv)) and the Ti–Ti bond (which is observed only in one interaction case, shown in figure 1(d)(iii)), we can argue that the Ti–O bond is stronger than both O–O and Ti–Ti bonds. These results imply that the breaking of both O–O and Ti–Ti bonds and formation of Ti–O bonds make the $Ti_2 + O_2$ system energetically more stable. Finally, in the case of the $Ti_2 + 2O_2$ reaction, as illustrated in figure 1(e), bent TiO_2 and the ground state structure of Ti_2O_4 clusters can be directly obtained.

Up to now, we have discussed the formation of some small TiO and TiO_2 clusters. Notice that it is relatively easy to find the global minimum structures of stoichiometric small Ti_nO_{2n} clusters for $n < 4$ (where n is the number of Ti atoms in the cluster) and our findings are consistent with previous experimental and theoretical works [53, 54]. In contrast, it is not an easy task to find true ground state structures for the large clusters, since the number of possible formation or growth paths increases enormously as the cluster size grows. For the construction of larger clusters, it is impossible to follow the same growth strategy as applied to the bent TiO_2 cluster. Therefore, we have considered many different configurations (around 10) as the starting geometries for each n in order to find the ground state as well as metastable structures. However, we have introduced some critical criteria based on physical arguments, in order to reduce the number of possible initial cluster structures and so the computational costs, and obtain stable and metastable cluster structures: we have avoided O–O bonds, whose formation is quite unfavorable in TiO_2 clusters, undercoordinated Ti atoms (each Ti atom binds to at least four O atoms) in the large clusters (for instance $n > 4$) and more than two monovalent O atoms. The monovalent O atom binds only to a single Ti atom and the bond length is around 1.64 Å, which is at least 0.2 Å shorter than the Ti–O bond length for a multi-coordinated O atom. For the bonding analysis, Ti–O and Ti–Ti bonds exist if Ti–O and Ti–Ti interatomic distances are smaller than 2.13 and 2.94 Å, respectively. For the bulk anatase and rutile phases of TiO_2, Ti–O bond lengths range from 1.95 to 2.01 Å. The coordination number, defined as the total number of nearest neighbors of one Ti or O atom, is an important analysis tool for the investigation of the stability of the small titania clusters. Ti and O atoms are six- and threefold coordinated in bulk anatase and rutile. Also, the structures derived directly from bulk anatase and rutile geometry have been considered, at least for benchmarking purposes.

3.1. $(TiO_2)_n$ clusters for $n = 1$–5

We have determined the equilibrium structures of the clusters via total energy calculations without imposing any symmetry constraint. Figure 2 illustrates the optimized structure of the five lowest lying isomers for $n = 1$–5 clusters. Assigned labels (**na**, **nb**, etc) depicted in figure 2 are used in order to identify each of the clusters. **na** is the calculated ground state structure of the $(TiO_2)_n$ cluster. For $(TiO_2)_2$ clusters, **2a** is 0.26 eV lower in energy than its *cis* isomer **2b**. The third lowest lying isomer of $n = 2$ clusters, **2c**, has a cage which is formed

by three O atoms. Three- and fourfold coordinated Ti atoms occupy the apexes of this cage. Due to repulsive interaction which results from the cage geometry among three O atoms, **2c** is 0.56 eV higher in energy than the **2a** structure. In the case of $n = 3$ clusters, the calculated ground state structure has both threefold coordinated and monovalent O atoms. The energy difference between **3b** and **3c** isomers of $(TiO_2)_3$ is found to be very small. They might simultaneously exist in a TiO_2 cluster mixture. In reality, several isomers of a particular $(TiO_2)_n$ cluster are expected to be observed if the energy difference is small between them. Therefore, the free energy is the most crucial thermodynamical quantity in determining the lowest lying structures and ordering of the isomers of a particular cluster at finite temperatures. However, in this study, we have only dealt with calculated total energies and not the free energies of the clusters. In contrast to our results, Qu [54] have found that **3c** structure is 0.24 eV lower in energy than that of **3b**. Note that different simulations using different basis sets, especially localized basis sets, or exchange–correlation functionals might observe different ordering of the isomers of a particular cluster. In this work, we particularly make sure that all of the computational parameters are well converged and suitable for this type of study. **2a** and **3b** structures are related to each other. One can form an infinite wire structure by repeated addition of TiO_2 bent molecules to the **2a** cluster. In each addition process, the calculated total energy per TiO_2 unit (E_T/m) increases and saturates as the value of m goes to infinity. Here, m and E_T represent the number of TiO_2 units and the total energy of the cluster, respectively. E_T/m is calculated as 23.61, 24.31 and 24.68 eV for **2a**, **3b** and **4d**, respectively, and it becomes 25.78 eV for the infinite chain wire. Even though two-dimensional (2D) structures do not obey our cluster construction criteria, we have also considered the planar clusters for comparison. All 2D clusters have a ring structure and the number of monovalent O atoms is set to n. Furthermore, Ti atoms bind to three O atoms. The total energy difference (E_{diff}) between the lowest lying structure of a particular cluster (E_{na}) and its planar isomer (E_{plnr}) decreases with decreasing n. For instance, E_{diff} ($=E_{plnr} - E_{na}$) is equal to 1.83, 2.82, 5.46 and 8.25 eV for $n = 3$, 4, 5 and 6 clusters, respectively. The calculated E_{diff} values are all positive, and this means that three-dimensional (3D) cluster structures are more stable compared to their 2D isomers. The formation of the 2D clusters becomes quite unfavorable as the size of the cluster grows. Normally, the formal oxidation states of O and Ti atoms are (−2) and (+4), respectively. In contrast to the 3D clusters, most of the O and Ti atoms in the 2D clusters do not reach their formal oxidation states, which lowers the stability of these planar structures. Notably, we have observed a different behavior as the planar clusters have been compared with each other. We have defined a ratio (E_T/n) between the total energy and corresponding n value of the planar clusters in order to understand the relative stabilities. The behavior of E_T/n is completely opposite to that of E_{diff}. The calculated E_T/n values are 23.82 (for $n = 3$), 23.98 (4), 24.04 (5) and 24.07 eV (6). The key point for explaining this different behavior is the O–O repulsive interaction, which mainly determines relative stabilities among 2D clusters. The ring radius of the planar clusters increases with n, which leads to a decrease in average interatomic distance between O atoms, thereby lowering the repulsive interaction.

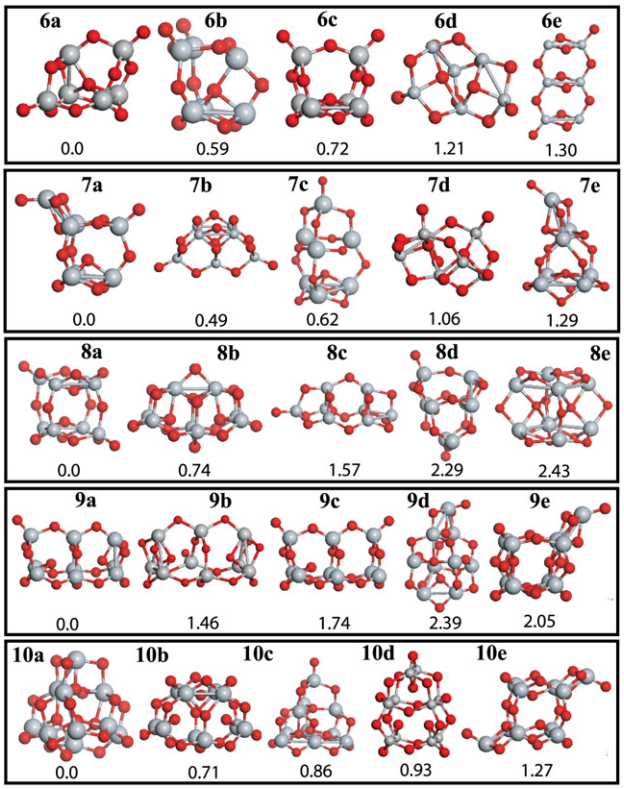

Figure 3. The same as figure 2 but now for $n = 6$–10 clusters.

In the case of $(TiO_2)_4$ clusters, the **4c** structure can be obtained from two **2a** structures. Similarly, one can also form an infinite wire structure by repeated addition of **2a** to the **4c** cluster in an appropriate way, and the emergent infinite structure has higher stability compared to both **2a** and **4c** clusters. Note that the global minimum **4a** has a fourfold coordinated O atom. Notwithstanding, in the study of Qu *et al*, the **4b** structure was found as the global minimum structure and the calculated energy difference between **4b** and **4c** was 0.29 eV. For the case of $n = 5$ clusters, both **5a** and **5b** structures have fourfold coordinated O atoms. The **5a** structure is 0.16 eV lower in energy than that of **5b**. The number of monovalent O atoms is two and one in **5a** and **5b** structures, respectively. We have also investigated the formation of **2a**, **3a** and **4a** from **1a**. If two **1a** interact in a suitable configuration, one can obtain **2a**. Similarly, **3a** (**4a**) can be formed by adding extra **1a** to **2a** (**3a**). In this way, the smaller clusters can be used as the building block of the larger systems.

3.2. $(TiO_2)_n$ clusters for $n = 6$–10

Figure 3 represents the clusters of $n = 6$–10. The **6a** structure has a fourfold coordinated O atom which locates at the center of the cage of **6a**. The bond length between this O and each nearest Ti atom is around 2.03 Å. **6b** and **6c** structures also have fourfold coordinated O atoms. Our lowest lying structure

6a is different from those of [54, 52, 53]. In the $n = 7$ case, **7a** is not the global minimum of [54]. The **7a** geometry is 0.49 eV more stable than the **7b**. All the lowest lying isomers have at least one monovalent O atom. There are two threefold coordinated O atoms in **7a**. We have found a new structure for the ground state of $n = 8$ clusters. **8a** has cubic-like structure. Two monovalent O atoms bind to inverse Ti atoms in opposite corners. **8b** and **8c** are the global minima of [54] and [52], respectively. **8d** and **9d** structures have been taken from the anatase crystal. Their energies are around 2.3 eV higher than both **8a** and **9a**. Therefore, we can argue that the ground state structures of the small TiO_2 clusters cannot be derived from bulk phases. Unlike $n \leq 8$ clusters, the ground state structure of $n = 9$ has only one monovalent O atom and it is 1.74 eV more stable than **9c**, which has two monovalent O atoms. **9a** and **9b** have one and two threefold coordinated O atoms, respectively. In contrast, **10a** possess no monovalent O atom. In the structure of **10a**, there are four fourfold coordinated O atoms and all Ti atoms have fourfold coordination. Note that the second lowest lying structure **10b** has also no monovalent O atom. **10a** is 0.93 eV more stable than the global minima of [55]. In general, the ground state structures in each n have at least one monovalent O atom.

Figure 4 shows the distribution of Ti–O, O–O and Ti–Ti interatomic distances for $n = 2$–10 clusters. Each atom is assigned as the center of a 4 Å radius circle and all interatomic distances between the central atom and other atoms which are inside the circle have been measured. This procedure has been performed for all the atoms in the cluster. The height of the peaks is proportional to the occurrence of a certain interatomic distance. We have divided each graph into three regions. The first region represents the interatomic distance between the monovalent O atom and its nearest Ti atom. It is seen that this bond distance appears as a very clear and distinct peak for $n = 1$–9 clusters, and these peaks occur around 1.64 Å. For the $n = 10$ cluster, there is no peak in the first region. In the second region, there are several peaks corresponding to the interatomic distances between multi-coordinated O atoms and their first nearest neighbor Ti atoms. We can also divide this region into three parts. Twofold coordinated O atoms are located near the first region. In the middle of the second region, both two- and threefold coordinated O atoms exist. In **3a**, the fourth peak is related to both two- and threefold coordinated O atoms. Finally, fourfold coordinated O atoms are close to the third region. Because of the low symmetry of the clusters, boundaries between these three parts are not so strict. We have a strong peak around 2.1 Å for fourfold coordinated O atoms in **10a**. The second peak in the $n = 2$ case exists for all n. In the third region, we have shown all other interatomic bond distances related to second, third, fourth, etc, nearest neighbors. For the small and relatively symmetric clusters such as **3a** and **10a**, almost all the peaks are very clear and distinguishable. In addition to Ti–O bonds, Ti–Ti bond lengths range from 2.72 to 2.94 Å and they are represented in the third region of figure 4. The coordination number of Ti and O atoms influences both Ti–Ti and Ti–O bond lengths. In the **2a** structure, the Ti–Ti interatomic bond distance is 2.72 Å. In this structure, Ti atoms bind to three

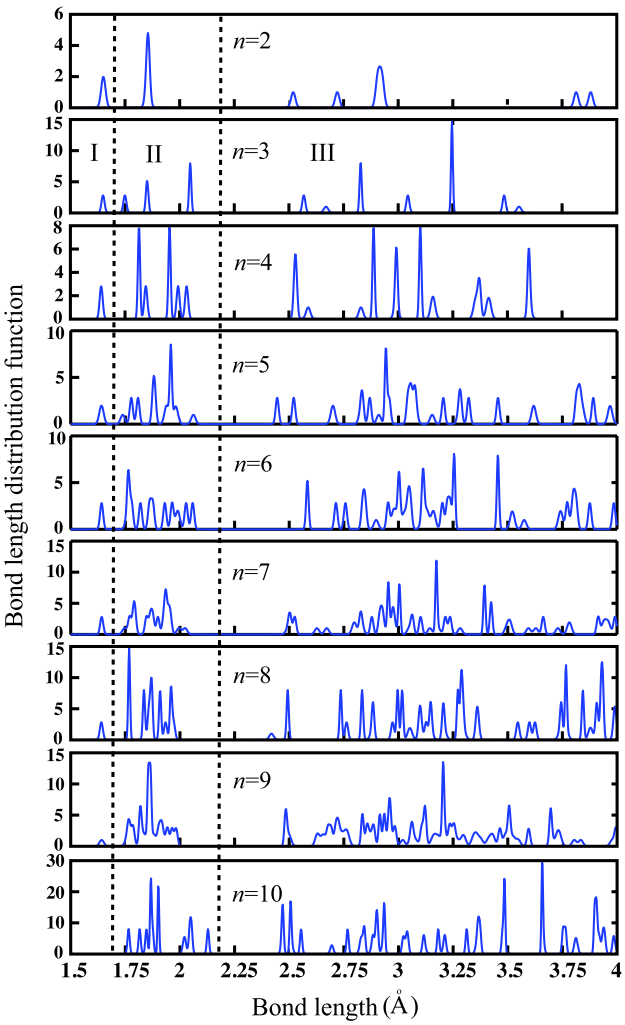

Figure 4. Gaussian smeared distribution of Ti–O, O–O and Ti–Ti interatomic distances for ground state geometries of $n = 2$–10 clusters. Two dashed lines divide the graphs into three regions. Region I, bond distance distribution between monovalent O and its nearest Ti atom; region II, distribution of the bonds between highly coordinated (at least two) O and first nearest neighbor Ti atoms; region III, assortment of second, third, fourth etc nearest neighbor interatomic distances. This region also includes the first and high order nearest neighbor distances between Ti atoms (Ti–Ti interatomic distance).

O atoms. Ti–Ti as well as Ti–O bond lengths increase as the coordination number of these atoms increases.

3.3. Stability of the $(TiO_2)_n$ clusters

In order to quantify the relative stabilities of these clusters, we have calculated the formation energy $E_f(=E_n/n - E_1)$ and nucleation energy $E_N(=E_{n+1} - (E_n + E_1))$ of the lowest lying structures. E_1, E_n and E_{n+1} are the total energies of the calculated ground state structures of TiO_2, $(TiO_2)_n$ and $(TiO_2)_{n+1}$ clusters, respectively. Figure 5(a) shows the formation energy per TiO_2 unit as a function of n. E_f is a measure of average energy per TiO_2 unit and indicates the stability of a particular cluster in terms of the $(TiO_2)_1$. All clusters ($n > 1$) have negative E_f and are stable with respect

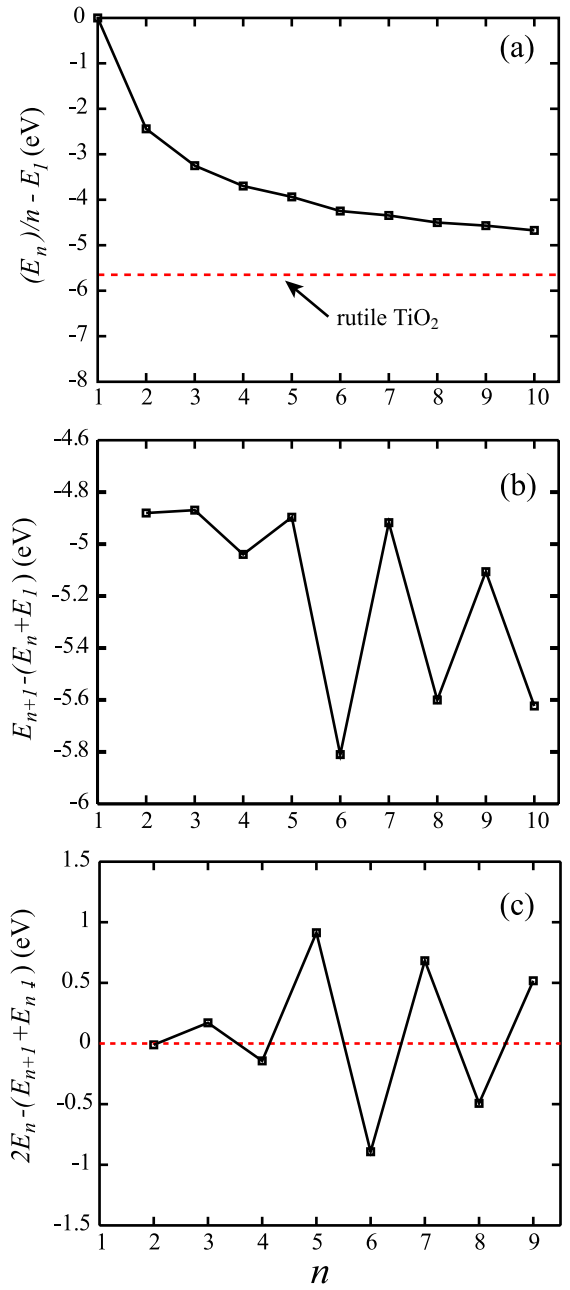

Figure 5. Formation energy ($E_f = E_n/n - E_1$) in (a), and nucleation energy ($E_N = E_{n+1} - (E_n + E_1)$) in (b) for the calculated ground state geometries. The second difference ($\Delta^2E = 2E_n - E_{n+1} - E_{n-1}$) in total energies of the clusters as a function of the cluster size (n) is given in (c).

to a single TiO_2 unit; see figure 5(a). In the same graph, we have also shown the formation energy of the rutile structure. The stability and possibility of formation of TiO_2 clusters can also be investigated by comparing E_f of these clusters with that of bulk phases of TiO_2. E_f approaches that of the rutile phase while the cluster size increases. It evolves as $E_f(n) = E_f$ (bulk rutile) $+ 5.56/n^{0.74}$, where E_f (bulk rutile) and $E_f(n)$ are theformation energy of the bulk rutile and the clusters, respectively. The energy difference between the formation energies of the bulk rutile and $(TiO_2)_{10}$ is 1.02 eV.

One can consider the formation of the larger clusters from the smallest unit ($n = 1$), as we have previously shown the growth mechanisms of some small clusters in figure 1. Figure 5(b) depicts the nucleation energy (E_N) of the clusters. E_N represents the energetics of the growth of $(TiO_2)_n$ from $(TiO_2)_1$ and $(TiO_2)_{n-1}$ clusters and exhibits an even–odd oscillation. From figure 5(b), we have noticed that the nucleation energy is less negative for odd n clusters. The growth of the even n clusters has been found to be easier than that of odd ones, and the fastest nucleation process has been observed in production of $(TiO_2)_6$ from $(TiO_2)_5$ and $(TiO_2)_1$. In a mixture of clusters having different sizes, $n = 6$ would be the most abundant one. Since some of our ground state structures are different from those obtained by Woodley *et al*, these results are in contradiction with [53]. According to their results, odd clusters are easy to form and abundance is the highest in $n = 5$ and 7 cases.

The second difference (Δ^2E) in total energies of the clusters is depicted in figure 5(c) and it has been calculated using the following expression: $\Delta^2E = 2E_n - E_{n+1} - E_{n-1}$. Δ^2E reflects the relative stability of the investigated cluster (n) with respect to its neighbors ($n - 1$ and $n + 1$) and can directly be compared with the relative abundances of the clusters determined in mass spectroscopy experiments. Positive (negative) Δ^2E means an unstable (stable) cluster with respect to its neighbors. Apparently, Δ^2E exhibits a clear even–odd oscillation with increasing n. As expected, Δ^2E is negative for even n clusters and this further verifies the stability of even clusters compared to odd ones. The $n = 6$ cluster has the lowest Δ^2E. Local minima have been found at $n = 2, 6, 8$, which indicates that these three clusters are more stable than their neighbors.

3.4. Electronic properties of the clusters

So far, we have discussed the structural properties and the stability of the titania clusters. Next, we have calculated the highest occupied molecular orbital (HOMO)–lowest unoccupied molecular orbital (LUMO) gap (E_g) of the lowest lying structures of all clusters in order to elucidate the electronic properties. Figure 6 shows the energy of HOMO and LUMO levels as well as their differences. As a consequence of the quantum confinement effect, which is crucial in nanosize particles, the HOMO–LUMO gap (E_g) decreases as the material size grows. However, we have not found any correlation between E_g and size of the clusters. The calculated E_g values are much dispersed. In general, the quantum size effect emerges from confinement. However, here, we have very small titania clusters, and we have observed that the structure of the clusters as well as the formation of monovalent O atoms plays an important role in determining the electronic properties, since the corresponding orbitals are often localized on the surfaces and, thus, that their energies depend critically on the surface structures. Therefore, it is impossible to relate these structures to bulk rutile, anatase or other bulk phases of TiO_2. Moreover, the clusters studied in this work are not crystalline. Satoh *et al* have experimentally shown that crystallinity of anatase TiO_2 nanocrystals (NCs) influences observation of quantum size effects [89]. Iacomino

et al have pointed out that the blueshift of the band gap of anatase NCs with respect to bulk anatase and the shape of the density of states depend on the NCs' crystallinity, the structural relaxation, and the surface properties [90]. Peng *et al* have investigated the electronic structure of passivated rutile quantum dots (QDs) [91]. According to their results, the band gap of the QDs evolves as E_g (QD) $= E_g$ (bulk rutile) $+ 73.70/d^{1.93}$. Here, E_g (QD) and E_g (bulk rutile) are the band gap of the QD and bulk rutile, and d stands for the diameter of the QDs. Notice that QDs have a wider band gap compared to the rutile bulk. Furthermore, in an experimental study [92], no quantum confinement effect has been observed for TiO_2 nanoparticles down to 1 nm, which is the exciton radius of TiO_2. In the study of Zhai *et al* [44], the band gap of a single negatively charged cluster approaches the bulk band gap limit when $n = 6$ and remains constant for $n = 6$–10. Our calculated E_{gap} values are 1.90 (3.03) eV for rutile and 2.30 (3.2) eV for anatase. The experimental values [16, 17] are quoted in parentheses. The calculated E_g of the $n = 3$ cluster is smaller than both E_{gap} of anatase and rutile. Although the sizes of our clusters are suitable to observe the quantum size effect, this result is inconsistent with the quantum size argument, in which the band gap of small molecules must be larger than that of bulk. We have observed that the structure of the clusters plays an important role in determining the electronic properties of very small titania clusters. E_g values of even n clusters are greater than the calculated energy band gap of both rutile and anatase phases as well as $n = 1$, 3, 7 and 9 clusters. In general, there is a direct relation between the stability and E_g of the clusters, and a larger E_g implies a higher stability of a particular system. As expected, even n clusters are more stable compared to odd ones in our work. E_g takes the highest value in the **10a** cluster, which has been found to be the most stable structure. The E_g values range from the infrared (1.76 eV for $n = 3$) to ultraviolet region (3.51 eV for $n = 10$), and this property could lead to design of suitable materials for photovoltaic and photocatalytic applications of TiO_2 clusters. Note that it is well known that standard DFT fails to calculate the correct energy band gap (E_{gap}). To this end, we performed some more calculations on the electronic structure of the TiO_2 clusters by using more accurate methods, namely hybrid functional PBE0 and including quasi-particle corrections within the G_0W_0 scheme. The results of electronic structure calculations within these more accurate but much more expensive methods without repeating the structural optimization of the cluster structures are summarized in the inset of figure 6(b). As seen from this inset, while the absolute value of the HOMO–LUMO gap changes considerably, the behavior of the H–L gap with the cluster size is same for all three calculations.

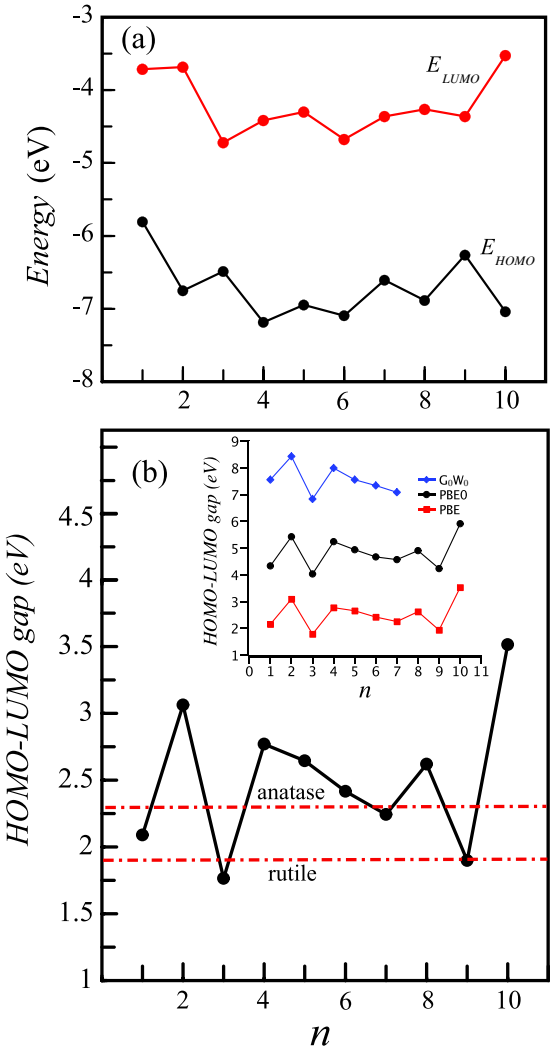

Figure 6. (a) Energies of HOMO (E_{HOMO}) and LUMO (E_{LUMO}) levels, and (b) their differences $E_{LUMO} - E_{HOMO}$, i.e. HOMO–LUMO band gap, or E_g. The calculated energy gaps of rutile and anatase are shown by red dotted–dashed lines. The inset shows the variation of E_g calculated from PBE0 and G0W0 as well.

3.5. Water adsorption

TiO_2 nanostructures are suitable candidates for water splitting and hydrogen production as a result of photovoltaic processes. Moreover, H_2O molecules almost always exist on the surfaces of TiO_2 nanoparticles. To understand the formation of TiO_2 nanoparticles produced under a wet process or dissociation of H_2O on TiO_2 surfaces, it is important to figure out the interaction between the H_2O molecule and zero-dimensional (OD), one-dimensional (1D) or 2D TiO_2 structures. In this study, we have also investigated the interaction of the ground state structures of the small titania clusters ($n = 1$–10) with a single H_2O molecule as well as multiple water molecules. For this purposes, we have considered three different adsorption modes: molecular adsorption, dissociative adsorption and H-bonding. For each case and each cluster size, we have tested at least four or five different orientations and configurations, especially looking at the cases where the O atom of water interacts with the Ti atom while the H atom of water interacts with the O atoms of the cluster. Figure 7 represents the optimized structure of the most favorable adsorption site for the single H_2O molecule on the selected clusters. Molecular adsorption of H_2O is common for all clusters. We have observed that the H_2O molecule preferentially binds to one of the Ti atoms, which retains no bound monovalent O atom.

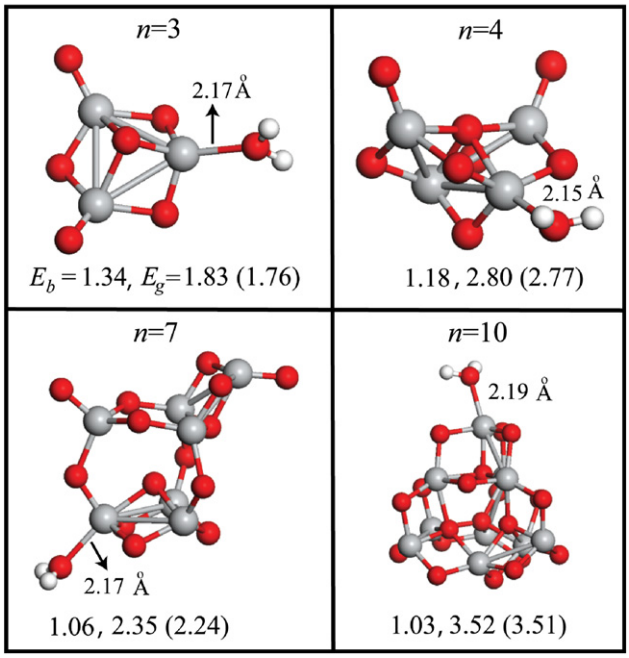

Figure 7. Optimized structure of the $H_2O + (TiO_2)_n$ system for the most favorable adsorption case of selected clusters. The binding energy E_b (first number) and the HOMO–LUMO gap (second number) are given for each cluster in eV. The values given in parentheses are the HOMO–LUMO gaps of the corresponding bare clusters.

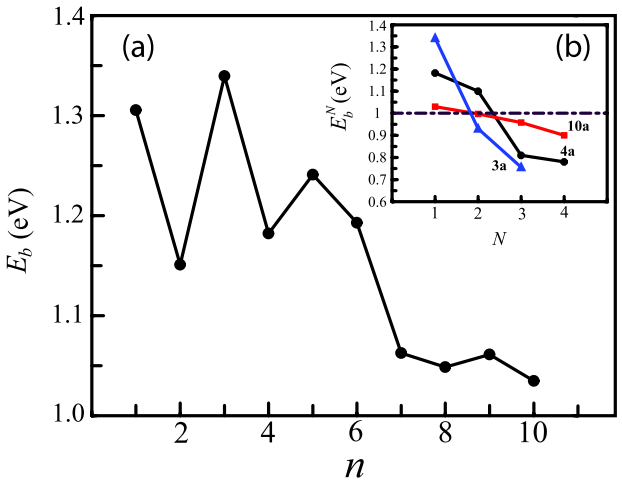

Figure 8. (a) Binding energy E_b between a single H_2O molecule and $(TiO_2)_n$ cluster as a function of n. (b) Variation of binding energy of the Nth H_2O molecule E_b^N on the $(TiO_2)_n$-$(H_2O)_{N-1}$ complex with the number of adsorbed H_2O molecules N for the **3a**, **4a** and **10a** structures.

Due to the stronger interaction of the lone electron pairs of the O atom with other materials compared to the H atom, the water molecule interacts with the titania cluster through its O atom. The interatomic distance between the Ti and O atoms is around 2.17 ± 0.02 Å. In figure 7, the binding energy (E_b) and HOMO–LUMO gap (E_g) for each system are also presented. We have defined E_b in terms of total energies of the isolated cluster, H_2O, and $(TiO_2)_n + H_2O$ complex, in the following form: $E_b = E_T[(TiO_2)_n] + E_T[H_2O] - E_T[(TiO_2)_n + H_2O]$. Figure 8(a) shows the variation of E_b of the single H_2O molecule as a function of the cluster size. We have two different binding regions. n ranges from 1 to 6 for the first region. The second region, which is approximately 0.1 eV lower in energy than the previous one, extends from $n = 7$ to 10. Notice that there is a sharp drop in E_b as n becomes 7. E_b oscillates as a function of n. For the $n = 1$–6 clusters, the amplitude of the oscillations is larger than those observed in $n = 7$–10 clusters. Even–odd oscillations observed in both regions are consistent with a general argument which can be outlined as the following: the reactivity (lower) of the clusters is related to their stability (larger). It is well known that the magnitude and shape of HOMO and LUMO levels as well as their differences have strong effects on the reactivity and chemical stability of a material. Similar to electronic properties of the bare clusters, the local structure of the binding sites of the water molecule and the structure of the clusters influence the interaction strength. E_b takes values ranging from 1.35 to 1.03 eV for the TiO_2 clusters studied here. The corresponding binding energy of molecular adsorption of H_2O on the rutile TiO_2(110) surface (modeled by a four layer 2×1 slab) is calculated as 0.73 eV in agreement with previous DFT studies [93–95]. Hence, the E_b of molecular adsorption of water on nanoparticles is larger than that on the clean rutile (110) surface, but approaches it with increasing cluster size. Furthermore, **10a** has the lowest E_b, which reflects the larger stability of this cluster compared to others. In addition, the LUMO level of this cluster has the highest energy. Meanwhile, its HOMO is slightly higher in energy than **4a**, which has the lowest energy HOMO level. The interaction is stronger for the $n = 1$–6 clusters. In both regions, E_b of the single water molecule on the odd n clusters is larger than that of the even n clusters.

On the other hand, molecular adsorption of water is not the only mode observed on titania surfaces. For instance, it has been shown that dissociative adsorption occurs on the (001) anatase surface [96, 97]. In the case of the (110) rutile surface, although the molecular adsorption mode is widely accepted, the E_b of dissociative adsorption is close [93–95]. In order to check this, we have considered the dissociative adsorption of H_2O on $n = 3$, 7 and 10 clusters as well. The dissociated structure, OH binding to the Ti atom while the H binds to the lower coordinated O atom near Ti, is energetically more stable than the molecular adsorption geometry, 0.76, 0.13 and 0.30 eV on $n = 3$, 7 and 10 clusters, respectively. However, dissociation is not exothermic. For example, the energy barrier for dissociation is around 0.5 eV on $(TiO_2)_3$ nanoparticles.

In practice, these nanostructures are expected to interact with many H_2O molecules. For this reason, we have examined the adsorption of multiple water molecules on **10a** as well as **3a** and **4a** structures to make a comparison between the clusters of different sizes. The number of possible adsorption sites for a molecule or an atom on clusters or nanoparticles increases as the surface area grows. The **10a** structure is the largest cluster in our study and has four possible Ti sites that can bind H_2O more strongly than other sites. Moreover, these Ti atoms have almost the same bonding environments. Figure 8(b) shows the variation of binding

energy of the subsequently adsorbed Nth H_2O molecule on the TiO_2–$(H_2O)_{N-1}$ complex as a function of the number of water molecules (N). The binding energy of each water molecule has been calculated as $E_b^N = E_T^{N-1} + E_T(H_2O) - E_T^N$, where E_b^N is the binding energy of the Nth water molecule on the cluster which has already adsorbed $N-1$ molecules. E_T^{N-1}, E_T^N, and $E_T(H_2O)$ are the calculated total energies of $(TiO_2)_{10}$-$(H_2O)_{N-1}$ and $(TiO_2)_{10}$–$(H_2O)_N$ complexes and the isolated water molecule, respectively. We have found that E_b^N decreases as N increases. The variation of E_b^N with the number of adsorbed water molecules in the **10a** case is almost linear. E_b^N for one molecule is 1.03 eV and it drops to 0.90 eV for the four H_2O case. The average interatomic bond distance between the O atom of the molecule and the Ti atom increases slightly and becomes 2.20 ± 0.02 Å for the four molecule case. For the **3a** and **4a** clusters, E_b^N drops more rapidly compared to the **10a** cluster. It is noticed that there is a crossover between E_b^N of **10a** and **3a** (and also **4a**). As N is greater than 1 (2) for **3a** (**4a**), water molecules bind to the **10a** cluster more strongly than to the smaller clusters. In **3a** and **4a** clusters, the bound water molecules are very close to each other compared to those in **10a**. Accordingly, the interaction between these smaller clusters and the next adsorbed molecule gets weaker with each adsorbed H_2O compared to the case in **10a**. Even though direct H_2O molecule–cluster interaction through a Ti–O bond with E_bs around 1 eV (so the bonding nature is more chemisorption-like) is strong, we have checked the adsorption of multiple H_2O molecules (up to four) on previously adsorbed water molecule(s) by means of H-bonding for $n = 3$, 4 and 10 nanoparticles. We have considered different orientations of the next water molecule approaching the adsorbed H_2O molecule or the surface of $(TiO_2)_n$. After all, on the $n = 3$ and 10 clusters, H_2O molecules adsorbed through separate Ti atoms of the cluster surface are at least 0.2 eV lower in energy compared to H_2O molecules binding to the cluster by means of H-bonding either directly to surface O atoms or to adsorbed water molecules. However, after two adsorbed H_2O molecules on the $n = 4$ case, the third and fourth ones each prefer to bind via two H-bonds with O atoms of the cluster surface and the adsorbed water molecule with an energy gain around 30 meV for each H-bond. From this example, we can argue that the coordination numbers of all four Ti atoms of the $n = 4$ cluster become similar with two adsorbed H_2O molecules by forming Ti–O bonds, and the $(2H_2O + (TiO_2)_4)$ conforms to a compact structure, so further incoming water molecules prefer H-bonding instead of a bond with saturated Ti atoms. Anyway, the energy difference between these two adsorption modes is very small, and the overall behavior displayed in figure 8(b) does not change at all.

Next, we have considered the effect of adsorption of a water molecule on the electronic properties of the bare clusters. Figure 9 represents the orbital energy levels of the clusters of $n = 3$, 4, 7, and 10 before and after the adsorption of the H_2O molecule. Due to the interaction, energy levels of the bare clusters shift to higher energies. The amount of shift in each level (ΔE) decreases as cluster size grows and there is a direct correlation between E_b and ΔE. Weak interaction

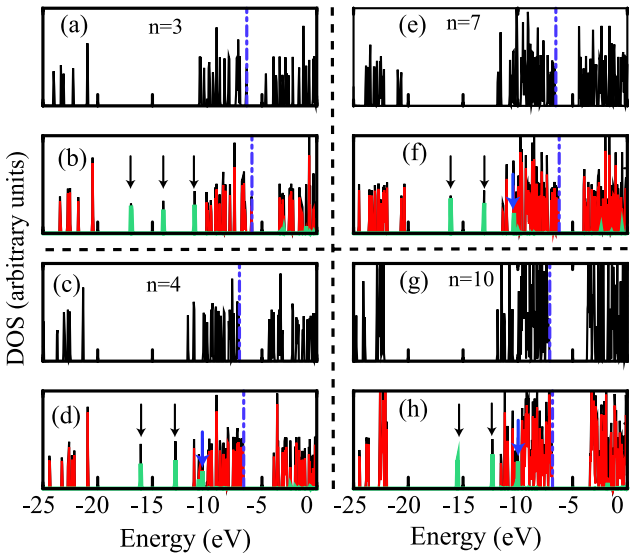

Figure 9. Electronic levels for $(TiO_2)_n$ ($n = 3$, 4, 7 and 10) clusters before ((a), (c), (e) and (g)) and after ((b), (d), (f) and (h)) the interaction with H_2O. The arrows show the positions of H_2O levels after adsorption on the clusters. The HOMO level is shown by the violet dot–dashed line. Dark (black) and light (red) colors represent the total and cluster energy levels of the cluster + H_2O system after the interaction with H_2O, respectively.

means small ΔE. In figure 7, we have shown both E_g of the H_2–$(TiO_2)_n$ complex and the corresponding bare $(TiO_2)_n$ cluster. Notice that the change in the E_g of the odd n clusters upon adsorption of the H_2O molecule are larger than those of the even n clusters. E_g increases from 1.76 to 1.83 eV in the case of $n = 3$, while we have observed a very small change (0.01 eV) for the $n = 10$ cluster case.

3.6. Transition metal adsorption

Ferromagnetic semiconductors are potential materials for spintronic applications. Transition metal (TM) doped TiO_2 has received considerable attention in the last several years to obtain ferromagnetism and efficient injection of spin-polarized carriers for semiconductor spintronic devices [98–107]. Furthermore, metal doped TiO_2 nanomaterials have been extensively investigated in order to improve photocatalytic performance of bare titanium dioxide nanostructures for several promising applications such as water splitting and degradation of various organic pollutants [3]. Therefore, a systematic study of adsorption of metal atoms on TiO_2 clusters becomes a significant aim for both scientific and technological viewpoints. In this part, adsorption of three different TM atoms (Co, V and Pt) on TiO_2 clusters has been studied for the possibility of functionalization of these nanoscale structures. We have chosen $(TiO_2)_{10}$, which is the largest cluster in our study, as a prototype. Several different possible adsorption configurations have been considered in order to explore the most energetic adsorption sites. Mostly, we tried O-rich cluster geometries for the incorporation of the transition metal atoms without excluding the low-coordinated structures, since metal atoms usually

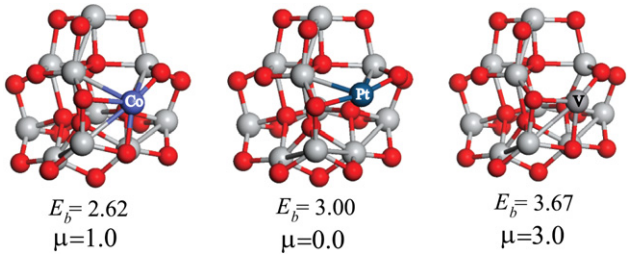

Figure 10. Most energetic adsorption site of Co, Pt, and V atoms on the $n = 10$ cluster. The corresponding binding energy E_b (in eV) and induced magnetic moment μ (in terms of μ_B) are also presented.

interact with O atoms of the TiO_2 clusters. In figure 10, we have shown the most favorable adsorption site for each TM atom. Adsorbates prefer special sites where they bind to many more cluster atoms compared to other possible adsorption sites. The binding energy (E_b) of the adsorbate atom has been obtained from the following expression: $E_b = E_T[(TiO_2)_{10}] + E_T[TM] - E_T[TM - (TiO_2)_{10}]$. Here, $E_T[(TiO_2)_{10}]$ stands for the total energy of the fully optimized bare cluster. $E_T[TM]$ is the energy of the isolated TM atom and $E_T[TM - (TiO_2)_{10}]$ represents the fully relaxed total energy of the single TM adsorbate on the cluster. TM atoms have found to interact strongly with the bare $(TiO_2)_{10}$ cluster. E_b has been calculated as 3.67, 2.63 and 3.0 eV for V, Co and Pt atoms, respectively. Adsorption of V and Co atoms on the cluster causes the magnetization of the whole system (TM–$(TiO_2)_{10}$) with induced magnetic moments of $\mu = 1.0$ and 3.0 μ_B, respectively.

Figure 11(a) shows the electronic density of states of the TM–$(TiO_2)_{10}$ system. Notice that there is a spin polarization for the V and Co cases. However, symmetry between the spin up and spin down states of the cluster is not disturbed so much upon adsorption of the V and Co atoms. Energy levels originating from TM atoms mostly appear within the gap region of the cluster, which leads to a significant gap narrowing in the doped system. The V and Co states are close to the conduction band (CB) edge of the cluster, and they hybridize with the d states of the Ti atoms. The electronic and optical properties of the bare cluster are altered by these gap localized adsorbate electronic states which cause a large redshift in all adsorbate cases. In the bare cluster, we have only electronic transitions from occupied states to unoccupied states. For the doped system, it is possible to observe several different electronic transitions (if these are allowed), which can be classified as (i) transition between the d states of the TM atom, (ii) electronic transition from occupied states of the cluster to empty d states of the TM atom or TM atom d orbitals to the host cluster, and (iii) transition from occupied orbitals of the host system to its unoccupied orbitals. These electronic transitions are illustrated in figure 11(b). The existence of various optical transition mechanisms is useful for scientific and technological applications. In this way, a large portion of the solar spectrum can be used, and we can achieve visible light activity for TiO_2 based systems. Doping substantially reduces the band gap of the cluster. E_g is calculated as 3.51 eV for the bare cluster, while it has been found to be 0.48, 0.14 and 1.65 eV for $(TiO_2)_{10}$–Co, –V and –Pt, respectively. The HOMO level of the whole system arises predominantly from the dopant atoms. In the Co case, the HOMO level mainly consists of d_{x^2}, d_{z^2} and d_{yz} orbitals of the Co atom. For the LUMO level, we have both contributions from the d_{xy} orbital of Co and the d orbital of Ti atoms. For the V case, the HOMO and LUMO levels are close to each other, which leads to very small band gap compared to the Co and Pt cases. The spin polarizations of both levels are the same. All d orbitals of V contribute to different extents to the formation of the HOMO level of the whole system. The LUMO consists of d_{x^2}, d_{z^2} and d_{yz} orbitals. The Pt adsorbed cluster has paramagnetic ground

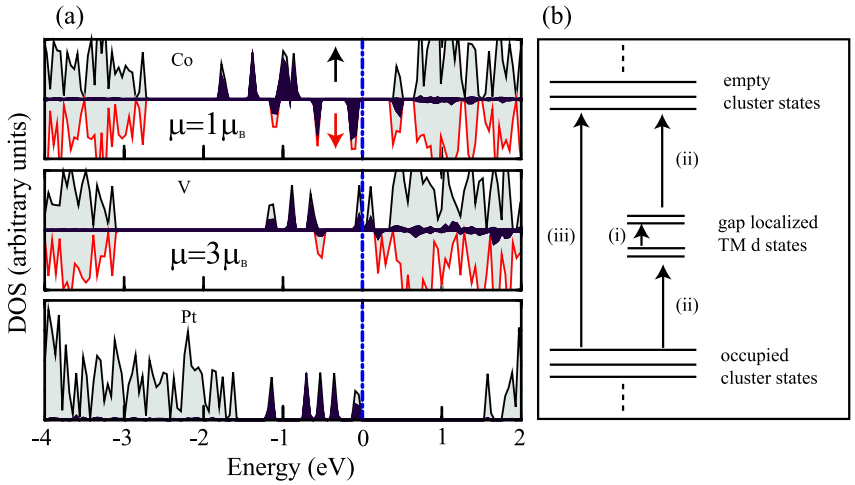

Figure 11. (a) Gaussian smeared density of states (DOS) of TM doped $(TiO_2)_{10}$ cluster for the most stable adsorption structure. The HOMO level shown by the dotted–dashed (blue) line marks the zero of energy. The DOSs of TM atoms are shown in dark (violet) shading, while the light (gray) one denotes the total DOS. The magnetic moments are also given for V and Co doped clusters. Dark (black) and light (red) arrows represent the up and down spins. (b) Schematic illustration of the possible optical transitions observed in the TM doped cluster. A description of (i), (ii), and (iii) is given in the text.

state. Unlike the Co and V cases, the d states of the Pt atom are close to occupied states of the cluster. Energy levels coming from Co atoms are more spread in the gap region of the cluster with respect to other dopants. These results suggest that the electronic, optical and magnetic properties of TiO_2 clusters can be manipulated by using appropriate transition metal atom doping.

4. Conclusions

In summary, we have studied the growth behavior, stability, structural, electronic, and magnetic properties of the bare TiO_2 clusters of different sizes and their interaction with H_2O and transition metals, namely Co, V, and Pt. Ground state structures and relative energies have been predicted for $(TiO_2)_n$, where $n = 1$–10. First of all, we have observed that the structure and the size of the clusters have prominent effects on the stability, electronic and chemical properties of these low dimensional structures. In general, clusters prefer to form 3D structures in their ground states. The stability of the bare clusters increases as the cluster size grows. According to the calculated E_f, E_N and Δ^2E values, even n clusters exhibit higher stability. The coordination of O and Ti atoms is an important criterion to explore the stability of the clusters. Except $n \leq 2$ clusters and monovalent O atoms, Ti and O atoms are at least fourfold and twofold coordinated in the lowest energy structures, respectively. In general, the lowest lying structure of $n \leq 9$ clusters always possesses at least one monovalent O atom. However, the $n = 10$ cluster does not have any monovalent O atom in its calculated lowest energy structure. The calculated HOMO–LUMO orbital energies and their differences, E_g, exhibit geometry and size dependence and do not follow a regular pattern. Generally, the band gap of a nanoscale material is larger than its bulk counterpart, due to the quantum size effect, and this band gap approaches the bulk gap value as the size of the material grows. However, we have not observed any quantum size effect in the small TiO_2 clusters which have been considered in this work. The alteration in the geometrical structure of these small titania clusters is the key factor determining their electronic structure. The interaction of such small systems with molecules or atoms such as the H_2O molecule or TM atoms is important for both understanding experimental results and developing new device applications by using these clusters. The interaction strength between a single H_2O molecule and the ground state structure of a particular cluster depends on the size of the cluster. We have observed an oscillatory decrease in the binding energy E_b of H_2O with the size of the clusters. In the case of multiple water molecule adsorption, E_b per H_2O molecule decreases with increasing number of adsorbed molecule N. The reduction in E_b per H_2O molecule is more pronounced for an $n = 3$ or 4 cluster compared to the $n = 10$ case. Finally, interaction of the $n = 10$ cluster with TM atoms has been studied. TM elements such as Pt, Co and V are strongly bound to the $(TiO_2)_{10}$ cluster. Among them, Co and V induce magnetic moment. The optical performance of bare TiO_2 clusters under visible light can be improved by doping with TM atoms. E_g values of the TM doped $(TiO_2)_{10}$ cluster are significantly smaller than that of the bare cluster. The electronic, optical and magnetic properties of titania clusters can be tuned by using suitable dopants.

Acknowledgments

We acknowledge the support from TÜBİTAK, the Scientific and Technological Research Council of Turkey (grant no TBAG 110T394). Computing resources used in this work were provided by the National Center for High Performance Computing of Turkey (UYBHM) under grant number 10362008 (TÜBİTAK). OG acknowledges the support of the Turkish Academy of Sciences, TÜBA.

References

[1] Diebold U 2003 *Surf. Sci. Rep.* **48** 53–229
[2] Thompson T L and Yates J T 2006 *Chem. Rev.* **106** 4428–53
[3] Chen X and Mao S S 2007 *Chem. Rev.* **107** 2891–959
[4] O'Regan B and Grätzel M 1991 *Nature* **353** 737–40
[5] Grätzel M 2001 *Nature* **414** 338–44
[6] Grätzel M 2003 *J. Photochem. Photobiol.* C **4** 145–53
[7] Hagfeldt A and Grätzel M 1995 *Chem. Rev.* **95** 49–68
[8] Çakır D, Gülseren O, Mete E and Ellialtıoğlu Ş 2009 *Phys. Rev.* B **80** 035431
[9] Wu N-L, Wang S-Y and Rusakova I A 1999 *Science* **285** 1375–7
[10] Agrios A G and Pichat P 2005 *J. Appl. Electrochem.* **35** 655–63
[11] Hoffmann M R, Martin S T, Choi W and Bahnemann D W 1995 *Chem. Rev.* **95** 69–96
[12] Fujishima A and Honda K 1972 *Nature* **238** 37–8
[13] Fujishima A, Hashimoto K and Watanabe H 1997 TiO_2 *Photocatalysis: Fundamentals and Applications* (Tokyo: BKC)
[14] Wang R, Hashimoto K, Fujishima A, Chikuni M, Kojima E, Kitamura A, Shimohigoshi M and Watanabe T 1997 *Nature* **388** 431–2
[15] Sunada K, Kikuchi Y, Hashimoto K and Fujishima A 1998 *Environ. Sci. Technol.* **32** 726–8
[16] Tang H, Levy F, Berger H and Schmid P E 1995 *Phys. Rev.* B **52** 7771–4
[17] Emeline A V, Kataeva G V, Ryabchuk V K and Serpone N 1999 *J. Phys. Chem.* B **103** 9190–9
[18] Mete E, Uner D, Gülseren O and Ellialtıoğlu Ş 2009 *Phys. Rev.* B **79** 125418
[19] Mete E, Gülseren O and Ellialtıoğlu Ş 2009 *Phys. Rev.* B **80** 035422
[20] Anpo M, Kishiguchi S, Ichihashi Y, Takeuchi M, Yamashita H, Ikeue K, Morin B, Davidson A and Che M 2001 *Res. Chem. Intermed.* **27** 459–67
[21] Anpo M 2000 *Pure Appl. Chem.* **72** 1787–92
[22] Anpo M 2000 *Pure Appl. Chem.* **72** 1265–70
[23] Anpo M and Takeuchi M 2001 *Int. J. Photoenergy* **3** 89–94
[24] Anpo M and Takeuchi M 2003 *J. Catal.* **216** 505–16
[25] Takeuchi M, Yamashita H, Matsuoka M, Anpo M, Hirao T, Itoh N and Iwamoto N 2000 *Catal. Lett.* **67** 135–7
[26] Asahi R, Morikawa T, Ohwaki T, Aoki K and Taga Y 2001 *Science* **293** 269–71
[27] Khan S U M, Al-Shahry M and Ingler W B 2002 *Science* **297** 2243–5
[28] Valentin C D, Pacchioni G and Selloni A 2004 *Phys. Rev.* B **70** 085116
[29] Livraghi S, Paganini M C, Giamello E, Selloni A, Valentin C D and Pacchioni G 2006 *J. Am. Chem. Soc.* **128** 15666–71
[30] Valentin C D, Pacchioni G, Selloni A, Livraghi S and Giamello E 2005 *J. Phys. Chem.* B **109** 11414–449

[31] Valentin C D, Pacchioni G and Selloni A 2005 *Chem. Mater.* **17** 6656–65
[32] Lee J-Y, Park J and Cho J-H 2005 *Appl. Phys. Lett.* **87** 011904
[33] Çakır D and Gülseren O 2009 *Phys. Rev.* B **80** 125424
[34] Anpo M, Shima T, Kodama S and Kubokawa Y 1987 *J. Phys. Chem.* **91** 4305–10
[35] McIntyre N S, Thompson K R and Weltner W 1971 *J. Phys. Chem.* **75** 3243–9
[36] Balducci G, Gigli G and Guido M 1985 *J. Chem. Phys.* **83** 1909–12
[37] Balducci G, Gigli G and Guido M 1985 *J. Chem. Phys.* **83** 1913–6
[38] Yu W and Freas R B 1990 *J. Am. Chem. Soc.* **112** 7126–33
[39] Guo B C, Kerns K P and Castleman A W 1992 *Int. J. Mass Spectrom. Ion Processes* **117** 129–44
[40] Chertihin G V and Andrews L 1995 *Phys. Chem.* **99** 6356–66
[41] Wu H and Wang L-S 1997 *J. Chem. Phys.* **107** 8221–8
[42] Foltin M, Stueber G J and Bernstein E R 1999 *J. Chem. Phys.* **111** 9577–86
[43] Matsuda Y and Bernstein E R 2005 *J. Phys. Chem.* A **109** 314–9
[44] Zhai H J and Wang L S 2007 *J. Am. Chem. Soc.* **129** 3022–6
[45] Hagfeldt A, Bergström R, Siegbahn H O G and Lunell S 1993 *J. Phys. Chem.* **97** 12725–30
[46] Bergström R, Lunell S and Eriksson L A 1996 *Int. J. Quantum Chem.* **59** 427–43
[47] Walsh M B, King R A and Schaefer H F 1999 *J. Chem. Phys.* **110** 5224–30
[48] Albaret T, Finocchi F and Noguera C 1999 *Faraday Discuss.* **114** 285–304
[49] Albaret T, Finocchi F and Noguera C 1999 *Appl. Surf. Sci.* **144/145** 672–6
[50] Albaret T, Finocchi F and Noguera C 2000 *J. Chem. Phys.* **113** 2238–49
[51] Jeong K S, Chang C, Sedlmayr E and Sülze D 2000 *J. Phys. B: At. Opt. Phys.* **33** 3417–30
[52] Hamad S, Catlow C R A, Woodley S M, Lago S and Mejias J A 2005 *J. Phys. Chem.* B **109** 15741–8
[53] Woodley S M, Hamad S, Mejias J A and Catlow C R A 2006 *J. Mater. Chem.* **16** 1927–33
[54] Qu Z-W and Kroes G-J 2006 *J. Phys. Chem.* B **110** 8998–9007
[55] Qu Z-W and Kroes G-J 2007 *J. Phys. Chem.* C **111** 16808–17
[56] Persson P, Gebhardt J C M and Lunell S 2003 *J. Phys. Chem.* B **107** 3336–9
[57] Lundqvist M J, Nilsing M, Persson P and Lunell S 2006 *Int. J. Quantum Chem.* **106** 3214–34
[58] Barnard A S, Erdin S, Lin Y, Zapol P and Halley J W 2006 *Phys. Rev.* B **73** 205405
[59] Li S and Dixon D A 2008 *J. Phys. Chem.* A **112** 6646–66
[60] Calatayud M, Maldonado L and Minot C 2008 *J. Phys. Chem.* C **112** 16087–95
[61] Calatayud M and Minot C 2009 *J. Phys. Chem.* C **113** 12186–94
[62] Bandyopadhyay I and Aikens C M 2011 *J. Phys. Chem.* A **115** 868–79
[63] Syzgantseva O A, Gonzalez-Navarrete P, Calatayud M, Bromley S and Minot C 2011 *J. Phys. Chem.* C **115** 15890–9
[64] Chiodo L, Salazar M, Romero A H, Laricchia S, Sala F D and Rubio A 2011 *J. Chem. Phys.* **135** 244704
[65] Marom N, Kim M and Chelikowsky J R 2012 *Phys. Rev. Lett.* **108** 106801
[66] Koparde V N and Cummings P T 2005 *J. Phys. Chem.* B **109** 24280–7
[67] Naicker P K, Cummings P T, Zhang H and Banfield J F 2005 *J. Phys. Chem.* B **109** 15243–9
[68] Hoang V V 2007 *Phys. State Solidi* **244** 1280–7
[69] Shevlin S A and Woodley S M 2010 *J. Phys. Chem.* C **114** 17333–43
[70] Persson P, Bergström R and Lunell S 2000 *J. Phys. Chem.* B **104** 10348–51
[71] De Angelis F, Tilocca A and Selloni A 2004 *J. Am. Chem. Soc.* **126** 15024–5
[72] Redfern P C, Zapol P, Curtiss L A, Rajh T and Thurnauer M C 2003 *J. Phys. Chem.* B **107** 11419–27
[73] Barnard A S, Zapol P and Curtiss L A 2005 *J. Chem. Theory Comput.* **1** 107–16
[74] Erdin S, Lin Y, Halley J W, Zapol P, Redfern P and Curtiss L 2007 *J. Electroanal. Chem.* **607** 147–57
[75] Koparde V N and Cummings P T 2007 *J. Phys. Chem.* C **111** 6920–6
[76] Wang T-H, Fang Z, Gist N W, Li S, Dixon D A and Gole J L 2011 *J. Phys. Chem.* C **115** 9344–60
[77] Payne M C, Teter M P, Allen D C, Arias T A and Joannopoulos J D 1992 *Rev. Mod. Phys.* **64** 1045–97
[78] Kresse G and Hafner J 1993 Numerical computations have been carried out by using VASP software *Phys Rev.* B **47** 558–61
Kresse G and Furthmüller J 1996 *Phys Rev.* B **54** 11169–86
[79] Kohn W and Sham L J 1965 *Phys. Rev.* **140** A1133–8
Hohenberg P and Kohn W 1964 *Phys. Rev.* **136** B864–71
[80] Blöchl P E 1994 *Phys. Rev.* B **50** 17953–79
[81] Kresse G and Joubert D 1999 *Phys. Rev.* B **59** 1758–75
[82] Perdew J P and Wang Y 1992 *Phys. Rev.* B **45** 13244–9
[83] Monkhorst H J and Pack J D 1976 *Phys. Rev.* B **13** 5188–92
[84] Methfessel M and Paxton A T 1989 *Phys. Rev.* B **40** 3616–21
[85] Abrahams S C and Bernstein J L 1971 *J. Chem. Phys.* **55** 3206–11
[86] Burdett J K, Hughbanks T, Miller G J, Richardson J W Jr and Smith J V 1987 *J. Am. Chem. Soc.* **109** 3639–46
[87] Howard C J, Sabine T M and Dickson F 1991 *Acta Crystallogr.* B **47** 462–8
[88] Huber K P and Herzberg G 1979 *In Molecular Spectra and Molecular Structure IV. Constants* (New York: Van Nostrand Reihold)
[89] Satoh N, Nakashima T, Kamikura K and Yamamoto K 2008 *Nature Nano.* **3** 106–11
[90] Iacomino A, Cantele G, Ninno D, Marri I and Ossicini S 2008 *Phys. Rev.* B **78** 075405
[91] Peng H, Li J, Li S S and Xia J B 2008 *J. Phys. Chem.* C **112** 13964–9
[92] Serpone N, Lawless D and Khairutdinov R 1995 *J. Phys. Chem.* **99** 16646–54
[93] Kamisaka H and Yamashita K 2007 *Surf. Sci.* **601** 4824–36
[94] Harris L A and Quong A A 2004 *Phys. Rev. Lett.* **93** 086105
[95] Hammer B, Wendt S and Besenbacher F 2010 *Top. Catal.* **53** 423–30
[96] Gong X-Q and Selloni A 2005 *J. Phys. Chem.* B **109** 19560–2
[97] Gong X-Q, Selloni A and Vittadini A 2006 *J. Phys. Chem.* B **110** 2804–11
[98] Matsumoto Y, Murakami M, Shono T, Hasegawa T, Fukumura T, Kawasaki M, Ahmet P, Chikyow T, Koshihara S-Y and Koinuma H 2001 *Science* **291** 854–6
[99] Park M S, Kwon S K and Min B I 2002 *Phys. Rev.* B **65** 161201
[100] Kim J-Y, Park J-H, Park B-G, Noh H-J, Oh S-J, Yang J S, Kim D-H, Bu S D, Noh T-W, Lin H-J, Hsieh H-H and Chen C T 2003 *Phys. Rev. Lett.* **90** 017401
[101] Yang Z, Liu G and Wu R 2003 *Phys. Rev.* B **67** 060402
[102] Geng W T and Kim K S 2003 *Phys. Rev.* B **68** 125203
[103] Hong N H, Sakai J and Hassini A 2004 *Appl. Phys. Lett.* **84** 2602–4
[104] Ye L H and Freeman A J 2006 *Phys. Rev.* B **73** 081304
[105] Du X, Li Q, Su H and Yang J 2006 *Phys. Rev.* B **74** 233201
[106] Balcells Ll, Frontera C, Sandiumenge F, Roig A, Martnez B, Kouam J and Monty C 2006 *Appl. Phys. Lett.* **89** 122501
[107] Wang X W, Gao X P, Li G R, Gao L, Yan T Y and Zhu H Y 2007 *Appl. Phys. Lett.* **91** 143102